

## A TIME-DOMAIN PROCESS FOR SINGLE TRACE INVERSION<sup>1</sup>

JOHN B. DuBOISE JR.<sup>2</sup>

### ABSTRACT

An algorithm is presented for sparse-spike trace inversion with a known wavelet. It performs a perturbation of the input trace to maximize the spikiness or optimize the "entropy" while honouring the seismic band information. It operates in the time domain by iteratively minimizing a nonlinear objective function of the trace elements.

Horizon controls are incorporated as a natural extension of the objective function. Application to an example trace illustrates the scope of possible inverse models that can be obtained without violating reasonable residual error limits.

Root-mean-square (rms) velocity controls, which manifest themselves mainly at very low frequencies, are applied in a second step by adjusting the amplitudes of the spikes. No significant increase in the seismic band residual error accompanies the adjustment.

The spiked traces are suitable for conversion to acoustic impedance or velocity models that match both the seismic band and the very low frequency band derived from root-mean-square (rms) velocity models or check shots.

### INTRODUCTION

The purpose of the trace-inversion process described in this paper is to find spiky trace reflection-coefficient models (optimized entropy) of the earth from processed seismic data traces such as those of a final migration. Lindseth (1979) showed that under appropriate assumptions about the density, for instance Gardner's relation (Gardner et al., 1974), such spiked traces are suitable for conversion to acoustic impedance or velocity models.

Like most trace-inversion processes, this one starts with the convolutional model. The wavelet is a source of ambiguity in that many different assumed wavelets convolved with a corresponding spike model will return new traces identical to the input traces. From the input traces alone, the wavelet-model pair that is most nearly correct can not be determined. Physical assumptions or information concerning either the earth model

or the wavelets can help resolve the ambiguity. For instance, Chi et al. (1984) developed a technique based on the assumption that the amplitudes of the reflectors can be described as the product of a zero-mean Gauss distribution and a Bernoulli distribution. They simultaneously derived both wavelets and corresponding spiked traces.

In addressing this subject by another method, Levy and Fullagar (1981) and Oldenburg et al. (1983) noted that wavelet derivation can be treated as a separate problem. After finding wavelets, one can design and apply appropriate inverse filters to the traces. The resulting wavelets make the traces easier to interpret or analyze with an inversion algorithm. In this paper, as in the paper of Oldenburg et al. (1983), it is assumed that the wavelet information was obtained during other steps of the processing.

Inversion algorithms can be designed to take multiples into account. For instance, Koltracht and Lancaster (1988) developed a trace-inversion process with feedback and thresholding that finds the multiples along with the spike events. They showed how unstable a trace inversion can be if strong multiples are present. In this paper, multiple elimination is assumed to be part of the wavelet processing that precedes the inversion.

Finally, seismic traces are band limited; therefore the information used for inversion is also limited. For example, with a sampling interval of 2 ms the Nyquist frequency is 250 Hz. For a seismic band from 10 to 60 Hz, only 20 percent of the full information band is available. The process described here deals primarily with the ambiguities caused by the limited bandwidth.

Levy and Fullagar (1981) and Oldenburg et al. (1983) developed a frequency-domain technique to convert the traces (processed to a sinc-function imbedded wavelet) to sparse-spike sequences. The process to be discussed in this paper has advantages that arise from the objective function it minimizes, particularly its time-domain representation. It is fast, and its operation is seamless; therefore, it can process arbitrarily long trace segments without segmentation. Infeasibilities occur only if extreme controls or unrealistically stringent limits are imposed.

<sup>1</sup>Presented at the C.S.E.G. National Convention, Calgary, Alberta, May 16, 1990. Manuscript received by the Editor July 17, 1990; revised manuscript received April 22, 1991.

<sup>2</sup>CogniSeis Development Inc., 2401 Portsmouth, Houston, Texas 77098

I would like to thank my employer, CogniSeis Development Inc., for permission to publish this work.

**THEORY**

Input traces must be conditioned to meet a number of requirements. First, they must be as free of multiple contamination and noise as possible. They must also be scaled properly, so that the spiking process yields reflection coefficients of acceptable amplitudes. Except for scaling, which is trivial, these requirements are generally among the goals of standard processing.

The process does not derive wavelets, but there are numerous ways to obtain them outside the inversion. Matching to well logs is appealing, because it incorporates new geophysical information not in the seismic traces. The implementation assumes a simple tapered sinc-function wavelet; so the wavelet is supplied indirectly by filtering the trace to change the wavelet to the required form.

The sparse-spike hypothesis adds what has been described by Rietsch (1988) as "soft" information to the model trace of spikes. This effectively expands the information band and reduces the effect of the remaining random noise by reducing the spike events to a necessary minimum. Minimizing the size and number of spikes of the spiked trace is functionally the same as optimizing "entropy", as proposed by Rietsch for trace inversion and by, for instance, Jaynes (1968) for other problems.

The sparse-spike hypothesis is motivated by our geologically based knowledge that many exploration provinces are characterized by the presence of few major events which appear clearly on a section. If the prospect area does not show identifiable events, seismic prospecting itself may not be appropriate. At the same time, the hypothesis helps focus attention on events that can be identified with high confidence. Sparse-spike model construction discriminates against low-energy, less credible spike events.

This inversion process has two stages. The first stage is a nonlinear time-domain perturbation of the input trace to a sparse-spike trace. The perturbation is an iterative minimization of an objective function called here the "deviation energy". The second stage applies rms or stacking velocity low-frequency controls.

The perturbed or spiked trace has a necessary characteristic, i.e., as long as enough nonzero samples are in the spiked trace, its convolution with the wavelet returns a close approximation of the input trace. The deviation energy is given by

$$D = \sum_{i=1}^N (S_i - \sum_{k=-L}^L T_{i-k} W_{k,i})^2 + \epsilon \sum_{i=1}^N T_i^2 + \beta \sum_{i=1}^N \log |T_i|, \quad (1)$$

where  $S$  is the input trace,  $T$  is the spiky trace,  $\epsilon$  is a small prewhitening factor,  $\beta$  is the positive parameter that determines how many spikes will be in the spiky trace,  $N$  is the trace length,  $L$  is one-half the wavelet length, and the  $W_{ij}$  are the elements of the (possibly time-variant) wavelet.

The first term is the time-domain expression of the error energy between the seismic trace and the spiked trace convolved with the wavelet. The second term is present to guarantee that a stable minimum of  $D$  exists. "Prewhitening" is added in "spiking deconvolution" for the same reason. The small positive quantity  $\epsilon$  is only as large as necessary to attain

stability. The presence of significant energy outside the seismic band in the input trace will prevent proper convergence. But increasing  $\epsilon$  restores stability.

The third term is an "inverse spikiness energy". Its special nonlinearity is the key to producing a spiky trace. It could have other forms such as

$$\beta \sum_{i=1}^N \sqrt{|T_i|}$$

Minimization of  $D$  with this as the third term also produces spiky traces, but the logarithmic expression requires a little less computer time, and its form is that of entropy.

The minimization of  $D$  is iterative. Sample by sample, the partial derivative of  $D$  with respect to each  $T_i$  is set to zero and solved for  $T_i$ , using prior values of the other elements of  $T$ . Although  $D$  is not linear, setting a partial derivative to zero yields a simple quadratic expression, and acceptable convergence can be attained after twenty-five passes over all the samples.

The minimization of  $D$  is robust and stable in that it always finds a solution, as long as the input trace has little energy outside the seismic band. The process can be thought of as repeated modified convolutions; it requires about the same computer time as thirty convolutions. Since it is a time-domain operation, no segmentation is required.

To a degree, the solution is not unique, because the very high-frequency components of the solution (well above the seismic band) depend on details of the minimization and on the initial  $T$ . This manifestation of the limited bandwidth limits the significance of the fine detail.

Although the implementation assumes stationary, cosine-tapered, sinc-function wavelets, no further analysis is required to use time-variant or complicated wavelets.

The number of spikes in  $T$  depends on  $\beta$ . If it is very small, nearly all the samples are spikes; if very large, very few are spikes. The number of spikes is sensitive enough to both the data and  $\beta$  that it is prudent to automatically adjust  $\beta$  to obtain an acceptable number of spikes. In practice, this stage of a useful inversion needs to produce about 90 percent as many spikes as there are frequency components in the seismic band. Table 1 and Figure 1 illustrate the dependence of the result on  $\beta$ .

In Figure 1, the window of operation is 0.2 to 0.708 s, with the input trace cosine-taper muted prior to the minimization of  $D$ . Trace 1 shows the wavelet and trace 2 is the input trace. Both

**Table 1.** Relationships among  $\beta$ , residual error and number of spikes in solutions of Figure 1.

Trace	Number of Spikes	% Residual Error	$\beta \times 10000$
3	39	.26	1.91
4	36	.41	2.38
5	31	.75	3.73
6	22	2.64	11.4
7	17	5.15	22.2
8	13	8.19	43.4

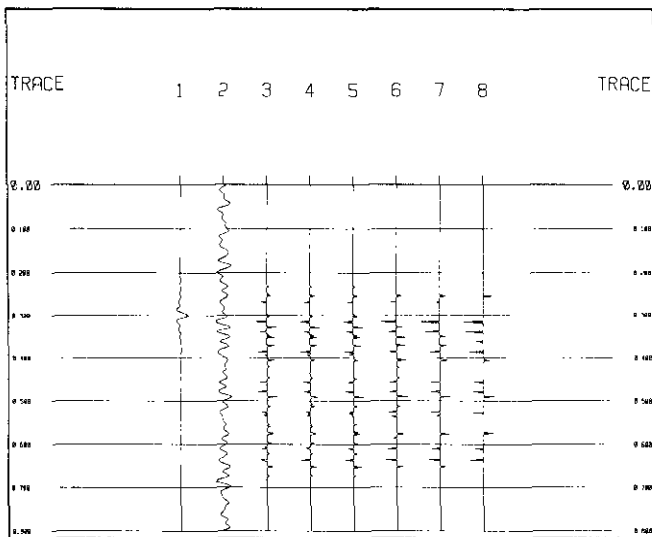


**Fig. 1.** Illustration of the process applied to a filtered noise trace. Trace 1 is the wavelet. Trace 2 is the filtered noise trace. Traces 3 through 8 are trace 2 inverted with increasing  $\beta$ .

have been rescaled to make them easier to see. Traces 3 through 8 are the spiked traces. Note that the residual error energy is small as long as the process produces an adequate number of spikes.

The spiked trace has a little less energy in the seismic band than the input trace. A normalization step follows the minimization to balance the seismic band energy.

**HORIZON CONTROLS**

Horizon controls are defined in terms of the relative velocities between layers after conversion of the reflection-coefficient traces to velocity. From the basic definition of the vertical incidence reflection coefficient, one can easily show that for small reflection coefficients

$$0.5 \log(Vd/Vs) = \sum_{i=J}^K T_i ,$$

where density is assumed constant,  $Vd$  is the interval velocity believed to characterize the deeper horizon, and  $Vs$  is that of the more shallow.  $J$  and  $K$  are end-point samples of the control horizons. Horizon-based controls are introduced by adding any number of extra terms of the following form to equation (1):

$$Wh(0.5 \log(Vd/Vs) - \sum_{i=J}^K T_i)^2 ,$$

where  $Wh$  is the weight assigned to the control. In general,  $Wh$  is set high enough that only an insignificant difference exists between the required trace element sum and the element sum after inversion. With these controls, the iterative minimization usually requires about four times as many iterations as the uncontrolled minimization.

It may not be possible to honour extreme horizon controls without significantly changing the seismic band frequency components. The closer the control horizons, the more serious this issue becomes. But control-horizon pairs of greater separation than about 80 ms for a wavelet such as that of trace 1 of

Figure 1 can generally be accommodated with residual errors of less than 5 percent.

Figures 2 and 3 illustrate the effect of applying controls. Trace 1 in Figure 2 is a random sequence filtered to the seismic band of 12 to 55 Hz. Trace 2 is trace 1 inverted, with a simple rms control applied after the minimization. Trace 3 is trace 1 inverted, with a horizon control designed to create the artificial acoustic impedance bulge from 0.6 to 0.75 seconds. Trace 4 is trace 1 inverted, with another horizon control to create a rough inverse of the artificial bulge of trace 3. Residual square errors of traces 2, 3 and 4 are 0.75, 1.13 and 0.52 percent, respectively. Figure 3 is Figure 2 converted to relative acoustic impedance by the approximate method of trace integration. Note the differences between the third and fourth traces of Figure 3.

Oldenburg et al. (1984) developed similar capabilities in their process. Their mathematical formulation led them to apply their controls as "constraints".

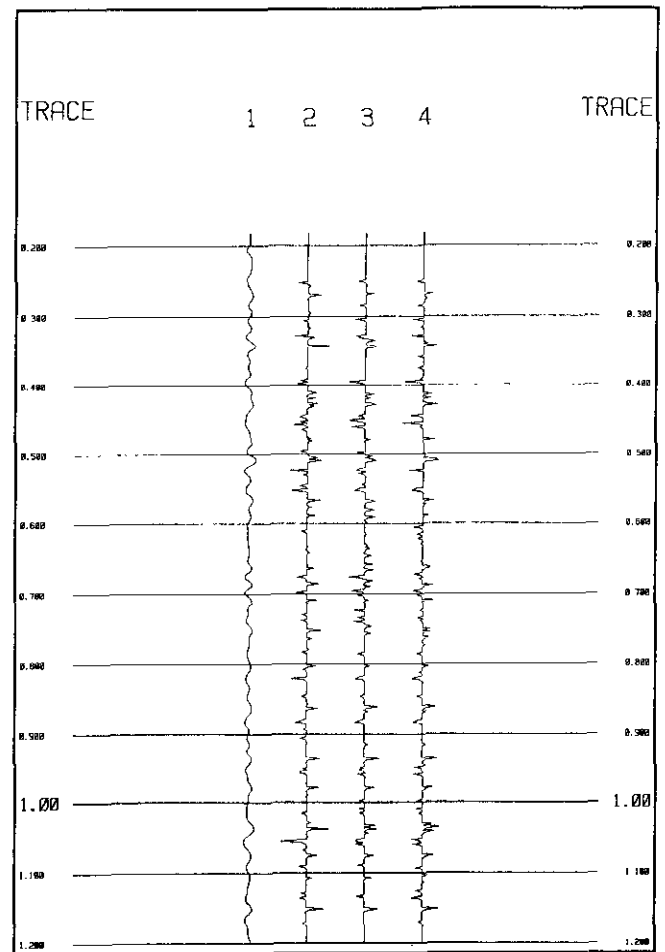


**Fig. 2.** Synthetic illustration of horizon controls. Trace 1 is a filtered noise trace. Trace 2 is its inversion without horizon controls. Trace 3 is trace 1 inverted with horizon controls to produce the bulge seen in trace 3 of Figure 3. Trace 4 is trace 1 inverted with horizon controls to produce a roughly opposite bulge to that of trace 3.

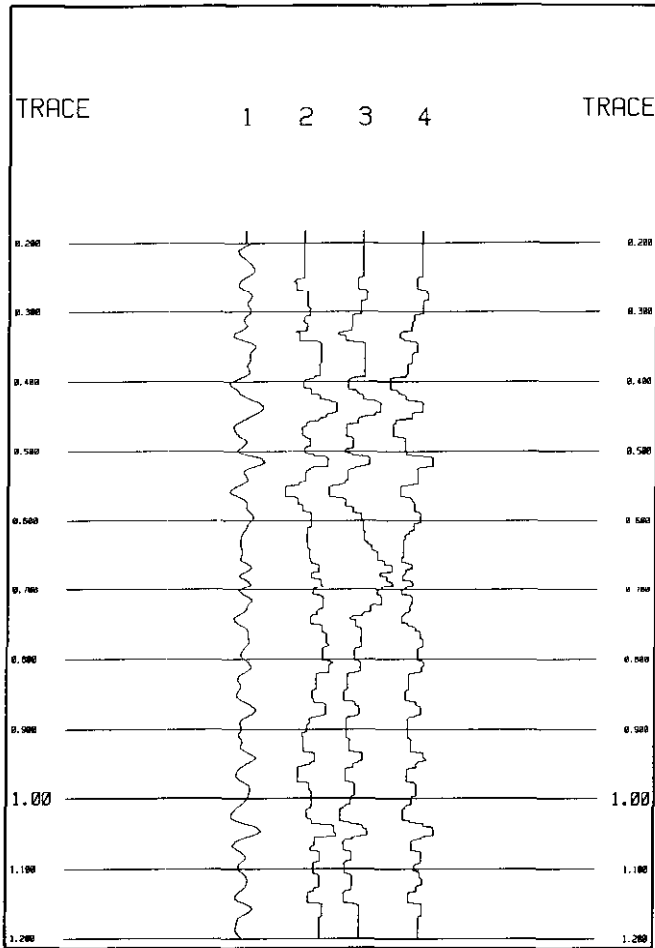


Fig. 3. Data shown in Figure 2 converted to relative impedance under assumption of constant density.

LOW-FREQUENCY CONTROLS

Far outside the seismic band, the perturbed, or spiked, traces display great variability from trace to trace. In the absence of comprehensive horizon controls, spectral components below 3 Hz will usually need to be corrected. In principle, this type of control could also be imposed by adding another term to equation (1). But the cost in computer time would be high. To avoid that cost, a second stage is introduced which involves minimization of another objective function of the spike amplitudes. This optional second stage of the overall process causes the low-frequency components to match rms velocity information. The low-frequency stabilization stage total square error is given by

$$E = \sum_{i=1}^M (T_i - A_i)^2 + Wr \sum_{k=1}^P [R_k - \sum_{i=1}^M A_i \cos(\omega_k L_i dt)]^2,$$

where  $M$  is the number of spikes,  $T_i$  is the spike amplitude derived in the first stage, and the  $A_i$  are the adjusted spike amplitudes.  $Wr$  is the weight assigned to the rms velocity information. Ordinarily, it is large.

The  $L_i$  are the spikes' locations.  $P$  is the number of rms cosine transform components,  $\omega_k$  is  $2\pi f_k$  (frequency) and  $dt$  is the

sample rate. The  $R_k$  are obtained from application of the standard Dix (1955) equation to a rms or stacking-velocity function to obtain a blocky interval velocity trace. Under the approximation of constant density, the interval velocity trace is converted to a reflection coefficient trace. The  $R_k$  are cosine transform elements of the reflection coefficient trace.

If sinc-function wavelets are used, the first term could be replaced by a term very similar to the second. In most cases, that modification will cause little change in the derived amplitudes of the spikes.

Since  $E$  is quadratic in all the  $A_i$ , its minimization is straightforward. The partial derivative of  $E$  with respect to each  $A_i$  is set to zero to obtain a set of linear simultaneous equations. The final spike amplitudes are their solution. Application of low-frequency controls increases the residual seismic band error. But since most of the effect is manifested well below the seismic band, the effect is minimal.

LOG DATA EXAMPLE

Figures 4 and 5 illustrate the performance of the process in recovering the important characteristics of a well log, using only the portion of its spectrum available in a seismic experiment. Trace 1, in Figure 4, is a reflection coefficient log from a test well. Trace 2 is trace 1 after application of a 10 to 60 Hz wavelet. Trace 3 is trace 2 inverted. Figure 5 is figure 4 converted to acoustic impedance.

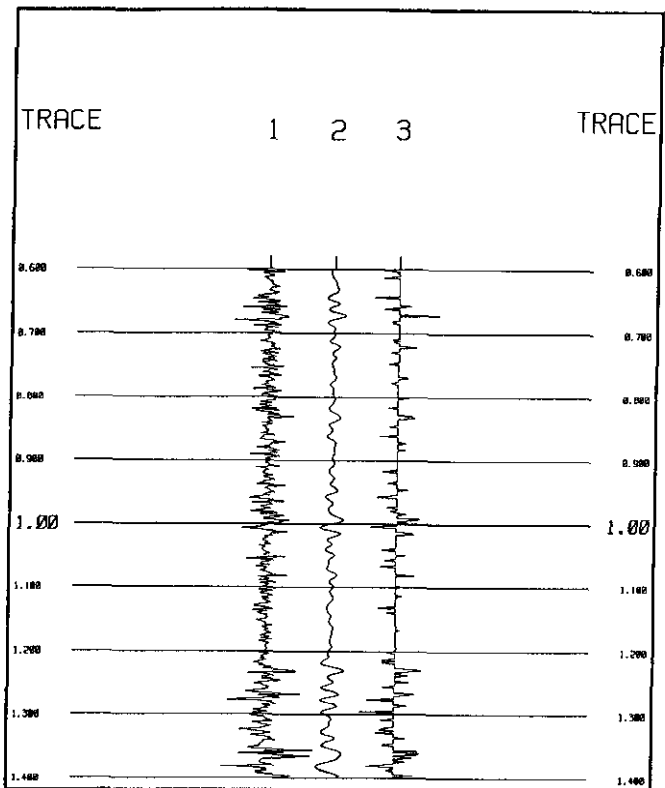


Fig. 4. Reflection coefficient log from a test well. Trace 1 is the RC log. Trace 2 is trace 1 filtered with the wavelet. Trace 3 is trace 2 inverted.

## CONCLUSION

A simple, computationally fast and stable trace-inversion process has been developed. It maximizes the spikiness or optimizes the "entropy" of the output trace while honouring the wavelet and the seismic band information.

Horizon controls can be introduced to force the derived velocity to match geological information about particular formations. And low-frequency rms or stacking velocity controls can be applied to impose a match to low-frequency interval velocity models obtained from check shots or stacking-velocity analysis.

## REFERENCES

- Chi, C-Y., Mendel, J.M. and Hampson, D., 1984, A computationally fast approach to maximum-likelihood deconvolution: *Geophysics* **49**, 550-565.
- Dix, C.H., 1955, Seismic velocities from surface measurements: *Geophysics* **20**, 68-86.
- Gardner, G.H.F., Gardner, L.W. and Gregory, A.R., 1974, Formation velocity and density — the diagnostic basics for stratigraphic traps: *Geophysics* **39**, 770-780.
- Jaynes, E.T., 1968, Prior probabilities: *Inst. Electr. Electron. Eng., Trans. Systems Science and Cybernetics* **SSC-4**, 227-241.
- Koltracht, I. and Lancaster, P., 1988, Threshold algorithms for the prediction of reflection coefficients in a layered medium: *Geophysics* **53**, 908-919.
- Levy, S. and Fullagar, P.K., 1981, Reconstruction of a sparse spike train from a portion of its spectrum and application to high-resolution deconvolution: *Geophysics* **46**, 1235-1243.
- Lindseth, R.O., 1979, Synthetic sonic logs — a process for stratigraphic interpretation: *Geophysics* **44**, 3-26.
- Oldenburg, D.W., Scheuer, T. and Levy, S., 1983, Recovery of the acoustic impedance from reflection seismograms: *Geophysics* **48**, 1318-1337.
- \_\_\_\_\_, Levy S. and Stinson, K., 1984, Root-mean-square velocities and recovery of the acoustic impedance: *Geophysics* **49**, 1653-1663.
- Rietsch, E., 1988, The maximum entropy approach to the inversion of one-dimensional seismograms: *Geophys. Prosp.* **36**, 365-382.

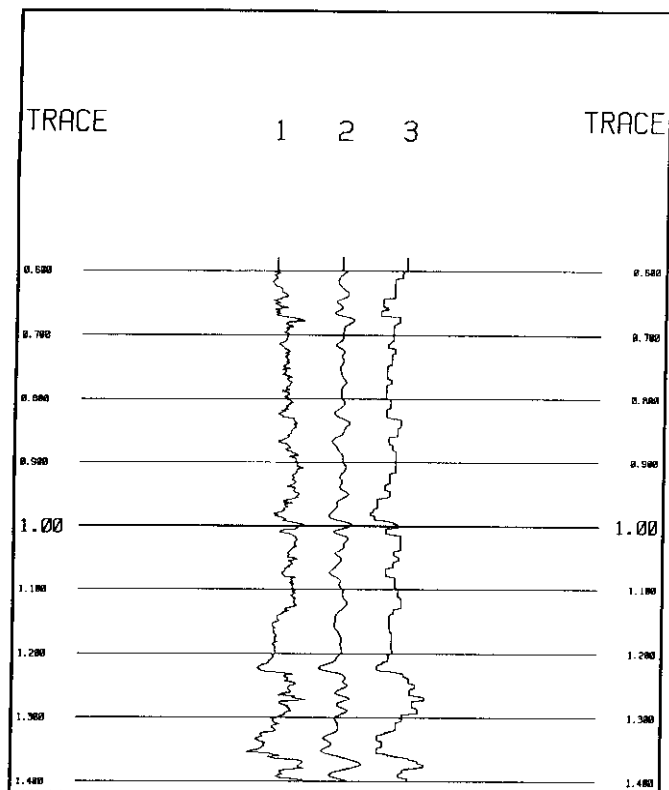


Fig. 5. Data shown in Figure 4 converted to relative impedance.

To the extent that this reflection coefficient log is the sparsest sequence of spikes consistent with its seismic band spectrum, trace 3 should be the same as trace 1. It is clear that this reflection coefficient log is not optimally sparse and that trace 3 falls short of matching trace 1. But in figure 5, trace 3 matches trace 1 better than trace 2, the result of not attempting a trace-spiking process. In general, the problems of matching well logs to seismic data cause greater discrepancies than are seen by comparing traces 1 and 3 in Figure 5.